Measurement and analysis of neutron spectra from a thick Ta target bombarded by 7.2*A* MeV ^{16}O ions

Maitreyee Nandy*
Saha Institute of Nuclear Physics, 1/AF, Bidhannagar, Calcutta 700 064, India

Tapas Bandyopadhyay† and P. K. Sarkar‡
Health Physics Unit, Variable Energy Cyclotron Centre, 1/AF, Bidhannagar, Calcutta 700 064, India
(Received 18 September 2000; published 20 February 2001)

Energy distributions of emitted neutrons were measured for 7.2*A* MeV ^{16}O ions incident on a thick ^{181}Ta target. Measurements were done at 0°, 30°, and 60° with respect to the projectile direction using the proton recoil scintillation technique. Comparison with calculated results from equilibrium and preequilibrium (PEQ) nuclear reaction models suggests the emission of PEQ neutrons at this projectile energy. This model also implies that PEQ emissions take place only before any scattering between target and projectile nucleons start. The paper discusses the method for selecting the initial exciton configuration with the help of measured data, and the stage at which the PEQ process is completed.

DOI: 10.1103/PhysRevC.63.034610 PACS number(s): 24.10.−i, 29.30.Hs, 25.70.−z

I. INTRODUCTION

Measurements of thick target neutron yield distributions from light or heavy ion induced nuclear reactions provide useful data for radiological safety and medical applications [1–3]. Additionally, an analysis of such data gives insights into the reaction mechnisms involved [1], even though the emitted spectrum from a thick target is a superposition of spectra from different stages of a continuously degrading projectile energy. The thickness of the target is so chosen that the projectile is completely stopped inside it. Thus it becomes feasible to make measurements at extreme forward angles with respect to the incident projectile direction. This is important since emission in the forward direction essentially carries the information about initial stages of the nuclear reaction mechanism.

We have measured neutron yield distributions from 7.2*A* MeV ^{16}O projectiles on a thick ^{181}Ta target at 0°, 30°, and 60° with respect to the projectile beam direction. The main purpose of these measurements is to investigate the occurrence of preequilibrium (PEQ) neutron emission from such a low projectile energy, particularly when the neutron separation energy from the target+projectile composite system in this case is around 8.9 MeV. We have analyzed the measured data using our earlier developed model [4] for estimating neutron emission from heavy ion collisions (HIC). This is done first of all to test our model at projectile energies around the threshold of PEQ emissions. In addition, we reexamine two aspects of PEQ reaction mechanism dealt in our earlier investigations [4,5]. The first one is about fixing the number of interaction stages necessary to complete the PEQ process to be followed by the equilibrium (EQ) emission process. The other one is about the selection of initial exciton number at the onset of HIC.

In Sec. II we describe our measurement procedure and data unfolding technique. Section III gives the procedure adopted to calculate thick target neutron yield distributions and a brief outline of the model used for the calculations. Details about the PEQ model used here are given in Ref. [4]. We present our experimental and theoretical results and discuss them in Sec. IV.

II. EXPERIMENTAL PROCEDURE

The measurements were carried out at the Variable Energy Cyclotron, Calcutta recently augmented with an electron cyclotron resonance (ECR) ion source. $^{16}O^{5+}$ ions accelerated to an energy of 7.2*A* MeV were incident on a thick target of ^{181}Ta. The Ta target, 4.0 ± 0.05 mm thick and 25 mm in diameter, was placed perpendicular to the beam axis. The thickness of the target was so chosen that the incident oxygen beam was completely stopped within the target while the scattering and absorption of the neutrons produced in the target were negligible. The energy distribution of neutrons emitted at angles 0°, 30°, and 60° with respect to the incident direction were measured with a 52.4 mm$\phi\times$52.4 mm NE-213 proton recoil liquid scintillator kept at a distance of 1.4 m from the target.

A collimator at a distance of 20 cm from the target was used to restrict the beam size. The beam was minimized at the collimator and maximized at the target so as to reduce the contribution of neutrons from the collimator to negligible proportions. Beam currents used for the present work were of the order of 5–15 particle nA.

In order to estimate the contribution from the room-scattered neutrons, a shadow bar was interposed between the target and the detector. The perspex shadow bar of length 100 cm and diameter 10 cm stops the primary neutrons from the target. The neutron spectrum measured with the interposed shadow bar gives the contribution of room-scattered neutrons which is subtracted from the original spectrum to obtain the corrected contribution.

The neutron spectra were calculated from the measured

*Electronic address: mnandy@hp2.saha.ernet.in
†Electronic address: tapas@veccal.ernet.in
‡Electronic address: pks@veccal.ernet.in

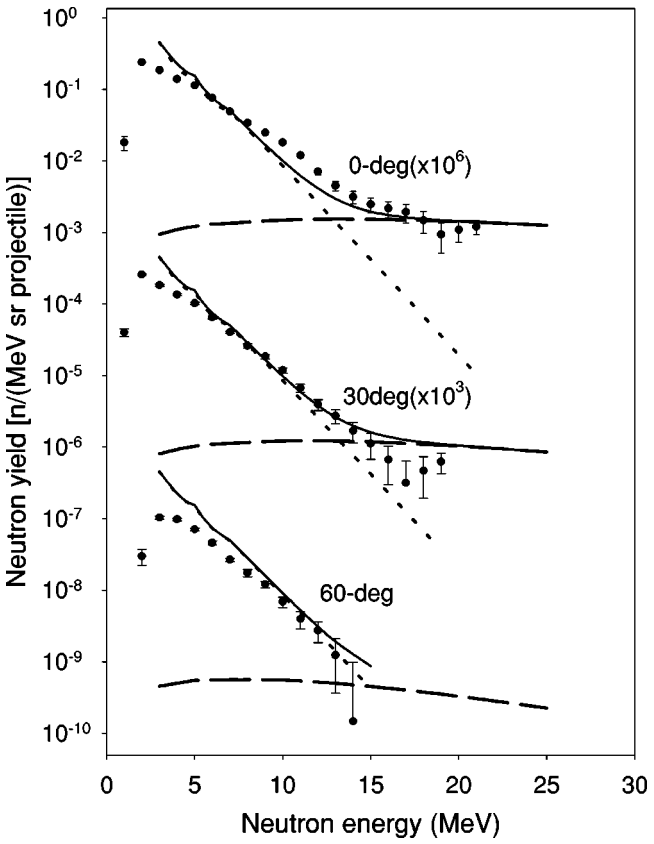

FIG. 1. Neutron yield distributions at 0°, 30°, and 60° for 7.2*A* MeV $^{16}O+^{181}Ta$. Measured data are shown as points with error bars. Calculated total (PEQ+EQ) distributions are shown as solid lines with PEQ component as dashed lines and EQ component as dotted lines.

pulse-height distributions with the help of the revised FERDO unfolding code [6] using the calculated (Monte Carlo) response functions. The energy differential neutron-yield distributions at emission angles 0°, 30°, and 60° are shown in Fig. 1 as points with errorbars. The total error associated with the unfolded spectra consists of (i) the statistical error associated with the measurement, (ii) the error arising from discretizing the continuous spectra and the response function, and (iii) the statistical error inherent in the Monte Carlo calculations.

III. MODEL CALCULATIONS

A. Thick target neutron yield distribution

In a thick target, the projectile interacts with the target nuclei at different, continuously degrading energies and the observed emitted spectrum is a sum of emissions from all these projectile energies within the target. For ease of calculations we have divided the thick target into a number of thin slabs such that the projectile loses a specified energy ΔE in each slab. The projectile is assumed to interact with all target nuclei in its path within this thin slab with an average energy. The slowing down is thus considered in small discrete steps. The emitted spectra from all of these slabs are summed up to give the final spectra. While considering the continuous slowing down of the projectile, we have ignored multiple scattering and straggling of the projectile as well as the scattering of the emitted neutrons in the target [1]. The kinetic energy E_P^i incident on the ith slab and the average energy in the ith slab $\overline{E_P^i}$ are given, for a projectile of energy E_P^0 incident on the thick target by

$$E_P^i = E_P^0 - (i-1)\Delta E,$$

$$\overline{E_P^i} = (E_P^i + E_P^{i+1})/2. \tag{1}$$

The slab thickness x_i is

$$x_i = \int_{E_P^i}^{E_P^{i+1}} \frac{dE}{-dE/dx}, \tag{2}$$

where dE/dx is the stopping power of the projectile in the target material that was calculated using the formalism of Zeigler *et al.* [7].

The neutron yield $\phi(\epsilon,\theta)d\epsilon d\theta$ at energy ϵ and direction θ with respect to the initial projectile direction is given by

$$\phi(\epsilon,\theta)d\epsilon d\theta = \sum_{i=1}^{m} \sigma(\overline{E_P^i};\epsilon,\theta)d\epsilon d\theta a_n x_i \times \exp\left\{-a_n\left[\sum_{k=1}^{i-1}\sigma_{fus}(\overline{E_P^k})x_k\right]\right\}, \tag{3}$$

where a_n is the number of target atoms per unit volume, $m = (E_P^0 - E_P^{th})/\Delta E$, E_P^{th} being the projectile threshold energy for neutron production. For $i=1$, the value of the exponential attenuation factor in Eq. (3) is taken to be unity. $\sigma(E_P;\epsilon,\theta)$ is the emission cross section of neutrons of energy ϵ at an angle θ when a projectile of energy E_P is incident on a target nucleus. Here, σ_{fus} is the fusion cross section of the projectile with the target.

B. Differential neutron emission cross section

The present experimental data were analyzed in terms of the PEQ and EQ models of neutron emission since for the projectile energy used in this experiment these two reaction types are expected to play significant roles.

The energy-angle differential neutron emission cross section for a projectile incident on a target nucleus with an energy E_P can be obtained as

$$\sigma(E_P;\epsilon,\theta)d\epsilon d\theta = \sigma_{PEQ}(E_P;\epsilon,\theta)d\epsilon d\theta + \sigma_{EQ}(E_P;\epsilon,\theta)d\epsilon d\theta, \tag{4}$$

where $\sigma_{PEQ}(E_P;\epsilon,\theta)$ and $\sigma_{EQ}(E_P;\epsilon,\theta)$ are, respectively, the cross sections of PEQ and EQ neutron emission in the direction θ with energy ϵ. In order to estimate the PEQ component we have used the formalism developed earlier [4,5]. The EQ emissions are calculated through Weisskopf-Ewing formalism as used in the code ALICE-91 [8].

1. PEQ emissions

The PEQ neutrons are emitted during the relaxation of the target + projectile composite nucleus as the total kinetic energy of relative motion of the two nuclei goes into excitation of the system. Relaxation of the composite system is described in terms of the number of stages N of two-body interactions in our PEQ model. After the relaxation process is complete and equilibrium is attained, EQ emission of neutrons takes place.

The double differential PEQ neutron emission cross section is given by

$$\sigma_{PEQ}(E_P;\epsilon,\theta)d\epsilon d\theta=\sigma_{fus}(E_P)\sum_N f_N^{\nu}\left[\frac{\lambda_C^{\nu}(\epsilon)}{\lambda_C^{\nu}(\epsilon)+\lambda_t^{\nu}(\epsilon)}\right]\times P_N(\epsilon,\theta)d\epsilon d\theta, \tag{5}$$

where f_N^{ν} is the number of excited neutrons after N two-body interactions. The term in the square brackets is the probability of emission of the neutron with energy ϵ from the composite system. The probability $P_N(\epsilon,\theta)d\epsilon d\theta$ is determined from the probability $P_N(E,\Theta)dEd\Theta$ of a particle moving inside the composite system with energy between E and $E+dE$ in the direction between Θ and $\Theta+d\Theta$ after N two-body interactions. The emission energy ϵ is related to the energy E by $\epsilon=E-E_0-S_{\nu}(C)$ where E_0 is the Fermi energy and $S_{\nu}(C)$ is the separation energy of a neutron from the composite nucleus. The direction θ outside the composite nucleus is related to the direction Θ inside it through the effects of refraction at the nuclear surface [9]. The probability $P_N(E,\Theta)dEd\Theta$ is obtained from the kinematics of two-body scattering inside the excited composite nucleus.

In nucleon induced reactions, the projectile is removed from the entrance channel and absorbed by the target through a two-body interaction with a target nucleon which is thereby raised above the Fermi level. This is the very first stage of interaction requiring the summation in Eq. (5) to start from $N=1$. But in heavy ion reactions, fusion of the projectile and the target starts through free flow of nucleons due to lowering of the potential barrier as the two reaction partners approach each other. For heavy ion induced reactions the summation in Eq. (5) starts from $N=0$ as particles may also be emitted without any two-body collision taking place [4]. The upper limit ($N_{\max}$) should be that value of N at which thermal equilibrium is reached and this was determined from kinematical studies.

(a) *Heavy ion fusion cross section.* We have calculated the fusion cross section for the ^{16}O projectile in ^{181}Ta using the formalism of Wilke *et al.* [10]. The fusion cross section is given by the classical expressions

$$\sigma_{fus}(E_{\text{c.m.}})=\begin{cases}\pi R_B^2\left(1-\dfrac{V(R_B)}{E_{\text{c.m.}}}\right), & \text{for} \quad E_{\text{c.m.}}<E_m\\ \pi\overline{\lambda^2}\left(l_{cr}+\dfrac{1}{2}\right)^2, & \text{for} \quad E_{\text{c.m.}}\geqslant E_m,\end{cases} \tag{6}$$

where $\overline{\lambda}$ is the de Broglie wavelength for the entrance channel, E_m coincides with the effective potential for the maximum critical angular momentum for fusion l_{cr} at barrier radius R_B and $V(R_B)$ is the total conservative potential at R_B. The values of l_{cr}, R_B, and $V(R_B)$ are taken from the tables in [10].

(b) *Excited particles at each interaction stage.* The number of excited neutrons for a given interaction stage N, f_N^{ν}, is calculated from the recurssion relation

$$f_N^{\nu}=f_{N-1}^{\nu}+f_{N-1}(P_N^{+}-P_N^{-})\left[\frac{A^{\nu}-f_{N-1}^{\nu}}{A-f_{N-1}}\right], \tag{7}$$

where P_N^{+} and P_N^{-} are, respectively, the total creation and annihilation probability in the Nth interaction [5] and f_{N-1} is the total number of excited particles of all type after $N-1$ interactions. A^{ν} is the total number of neutrons and A the number of neutrons+protons in the composite system. The detailed evaluation of P_N^{+} and P_N^{-} is given in Ref. [5].

Thus, at any stage f_N^{ν} can be determined if the number of excited neutrons at the initial stage $f_{N=0}^{\nu}$ is known. This number is given by

$$f_{N=0}^{\nu}=\frac{A_P^{\nu}}{A_P}f_{0P}+\frac{A_T^{\nu}}{A_T}f_{0T}, \tag{8}$$

where f_0 is the number of initial excited particles (neutrons +protons) and P and T in the subscript stand for contributions from projectile and target, respectively.

The number of initial excited particles f_0 is calculated from two different assumptions; one based on momentum space consideration [11], and the other [12] equating f_0 to the number of projectile nucleons A_P. In the first assumption we consider, in the c.m. frame of reference, an overlap of Fermi momentum spheres of the target, the projectile, and the composite system. The Fermi motions of the projectile and target nucleons are coupled with their c.m. motions [11]. The Fermi sphere of the composite nucleus is centred at the center of mass of the system. It is assumed that fusion starts when centres of the Fermi spheres of the projectile and the target are separated from that of the composite by the amount of their respective center-of-mass momentum per particle. The initial number of excited particles is determined from the momentum volume of the target and projectile Fermi spheres that remain outside the Fermi sphere of the composite nucleus. From the Fermi gas model, the density of the momentum states, $(\overline{n_i})$ is given by

$$\overline{n_i}=\frac{V_i}{2\pi^3h^3}=\frac{2r_0^3A_i}{3\pi^2h^3}, \tag{9}$$

where i stands for projectile or target and V_i is the relevant volume. Then the initial number of excited particles from the projectile or target is given by

$$f_{0i}=\overline{n_i}\int d\mathbf{p}, \tag{10}$$

with the integration carried out over appropriate limits of the momentum vector **p**.

In order to determine the distribution in energy and angle of these initial excited particles, the Fermi motions of the nucleons are coupled with the beam velocity in the laboratory frame. Thus for $N=0$, the distribution of f_{0P} particles excited from the projectile is obtained by coupling the Fermi velocity of these nucleons with the incident projectile velocity. The distribution of f_{0T} particles from the target is obtained by combining the Fermi velocity of these nucleons with the c.m. motion.

(c) *Distribution of the particles in the phase space.* In order to calculate the PEQ contribution the composite system is subdivided into two systems—a hot spot and a cold spot, which are described by a finite temperature and a zero temperature Fermi distribution, respectively, assuming partial equilibrium for each of them. The probability $P_N(E,\Theta)dEd\Theta$ is determined as the weighted sum of the scattering contributions from these two subsystems, i.e., (i) the probability of occupying the E,Θ state of the phase space through scattering between two particles in the hot spot and (ii) the contribution coming from the scattering of a particle in the hot spot with one in the cold spot. Details of this calculation are given in Ref. [4].

(d) *Emission probability and interaction rates.* The term in the square brackets of Eq. (5) is the emission probability of neutrons. In this expression, $\lambda_C^{\nu}(\epsilon)$ is the rate of emission with energy ϵ and $\lambda_t^{\nu}(\epsilon)$ is the rate of two body interactions of a neutron with other nucleons. The emission rate is given by [13]

$$\lambda_C^{\nu}(\epsilon)=\frac{(2s_{\nu}+1)m_{\nu}\epsilon\sigma_{inv}(\epsilon)}{\pi^2\hbar^3 g}, \tag{11}$$

where s_{ν} and m_{ν} are the spin and mass of a neutron, g is the single particle level density, and $\hbar=h/2\pi$. $\sigma_{inv}(\epsilon)$ is the cross section for the reverse reaction which is calculated by the method of Chatterjee *et al.* [14]. In estimating the two-body interaction rate, $\lambda_t^{\nu}(\epsilon)$, we have used the empirical relation of Blann [15]

$$\lambda_t^{\nu}(\epsilon)=[1.4\times10^{21}\{\epsilon+S_{\nu}(C)\}-6.0\times10^{18}\{\epsilon+S_{\nu}(C)\}^2]/k, \tag{12}$$

where k is an adjustable parameter for introducing the Pauli blocking effect. We have choosen $k=1.0$ in our calculations.

2. Evaporation calculation

The evaporation or EQ emission cross section is calculated using Weisskopf-Ewnig formalism in the ALICE-91 code. We have used the constant temperature level density expression of Gilbert and Cameron (GC) for lower excitation energies and the back-shifted Fermi gas expression for higher excitation energies. The transition energy, the nuclear temperature and the energy normalization factor of GC expression are obtained by matching the two level densities and their energy derivatives at the transition energy. The code ALICE-91 has been modified to include calculations with GC expression [16].

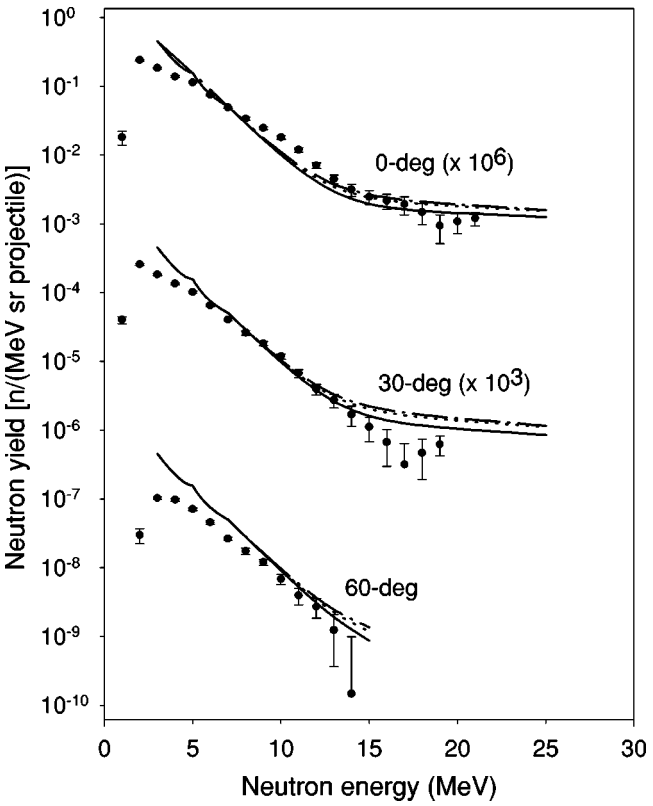

FIG. 2. Comparison of measured and calculated neutron yield distributions at 0°, 30°, and 60° for 7.2*A* MeV $^{16}O+^{181}Ta$. Calculated results are given for different choices of $N_{\max}=0$ (solid lines), 1 (dotted lines), and 2 (dashed lines).

IV. RESULTS AND DISCUSSION

Comparisons between theoretical calculations and the measured neutron yields at different laboratory angles are shown in Figs. 1–3 for various choices of the input options. The calculations are all done in the laboratory frame in which measurements were performed. For the present calculations, ΔE, the energy lost by the projectile in each thin slab [see Eq. (1)] was chosen to be 2 MeV. Slowing down of the projectile was considered down to 60 MeV (i.e., 3.75*A* MeV) below which σ_{fus} for the system becomes negligible.

Figure 1 shows the comparison of the experimental data with the calculated PEQ+EQ spectra (solid line) at 0°, 30°, and 60° laboratory angles. The PEQ and EQ contributions are also shown separately (dashed and dotted lines, respectively) at each angle. It can be observed that EQ emission alone does not account for the high energy part of the measured distribution. The discrepancy reduces with increasing angle of emission indicating presence of PEQ contributions in the neutron emission process. However, the contributions do not appear to be large though not insignificant. In evaluating the angular yield we have restricted the PEQ contribution to $N=0$ stage from the first slab only.

It is observed from Fig. 1 that the calculated neutron spectra give an overall good fit with the measured values at the three angles. But the compound nuclear emissions are slightly overpredicted at low emission energies at all angles,

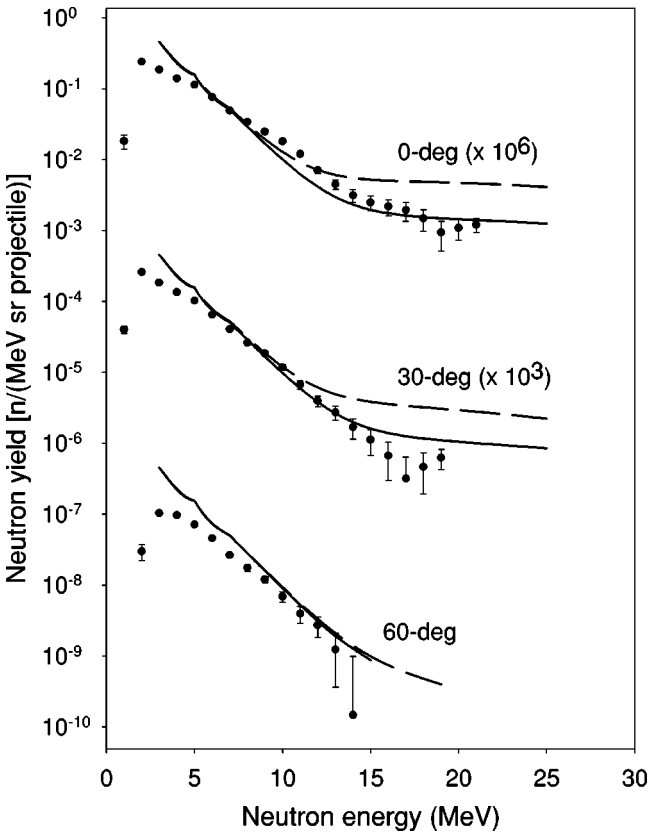

FIG. 3. Calculated results of neutron yield distributions at 0°, 30°, and 60° for 7.2*A* MeV ^{16}O + ^{181}Ta along with experimental data. Calculated results are for $f_0=A_p$ (dashed lines) and for f_0 as per Eq. (10) (solid lines).

with the discrepancy increasing at back angles. The overprediction may, then, be due to the choice of the level density parameter that plays a very important role in estimating the EQ emissions [4]. The high-energy neutron yield is well reproduced by the present calculation, except for a very small overprediction at 60°. Here again we see (as is evident from the figure) that the EQ component is overpredicted, the PEQ contribution is negligible at this angle for the beam energy considered.

We have studied the change in PEQ emission for different values of $N_{\max}$. This is done essentially to find the number of interaction stages N necessary to complete the relaxation process at such a low projectile energy. Figure 2 shows the calculated double-differential spectra against the measured ones at the three given angles for $N_{\max}=0$ (solid line), 1 (dotted line), and 2 (dashed line). For all the angles considered, it is observed that the PEQ emissions at energies above 10 MeV are slightly larger, when we take $N_{\max}=1$ instead of $N_{\max}=0$, the difference being greater for forward angles. Calculations with $N_{\max}=1$ overpredict the experimentally measured angular distributions. For interaction stages N greater than 1 the calculation shows negligible additional PEQ contributions. However, experimental evidence for this projectile energy seems to favor $N_{\max}=0$ indicating no PEQ emission after two-body interactions start between target and projectile nucleons.

In nuclear reaction model calculations of neutron emissions from nuclear interactions, it is not clear when to switch over to the EQ process from the PEQ. This problem has been addressed in an earlier work [5], where emphasis was given to the isotropic angular distribution of the emitted neutrons as a criterion for terminating the PEQ calculations. This led to the conclusion that about four interaction stages ($N_{\max}=4$) are needed in the present model to go over to the EQ calculations. However, in the same work while comparing the measured and calculated total PEQ multiplicity, it was seen (Fig. 1 of Ref. [5]) that for projectile energies around 10 MeV/nucleon, PEQ contributions can be restricted to $N_{\max}=1$. The present experiment also seems to support this observation of dependence of $N_{\max}$ on the projectile energy. However, inclusion of such dependence in the model calculation involves subjectivity as there is no way to estimate the value of $N_{\max}$ *a priori* for any projectile energy.

Now we turn our attention to the question of how any PEQ emission at all can take place at such a low projectile energy. The total excitation of the composite system is 81.7 MeV in this case. At the initial stage (before any two-body interaction) the number of excited particles is ten if we use Eq. (10) and it is 16 when we use $f_0=A_P$. This leads to a value of 8.17 MeV or 5.1 MeV per excited particle, respectively. Both these values are less than the separation energy of a neutron from the composite sytem (8.94 MeV). This can be explained as follows. We have considered that the fusion of the target and the projectile takes place just when the kinetic energy of the projectile is converted into the excitation of the composite system (overlap of nuclear potentials) creating a hot spot and a cold spot. The motion of nucleons inside the hot spot is described by coupling the velocity of the projectile with the nucleon velocites corresponding to a finite temperature Fermi distribution. As a result, a few of the excited nucleons attain energies higher than the separation energy even though the average energy of an excited nucleon is much lower. When two-body interactions take place, more nucleons are excited, thereby allowing the temperature of the hot spot to drop down as the size of the hot spot increases. The lower temperature Fermi distribution has much fewer nucleons above the separation energy restricting emissions from these stages. Crucial to this explanation is the assumption of finite temperature Fermi momentum distribution of the nucleons in the hot spot from the onset of the HIC. The present observations may be considered as a support of our assumption that a finite temperature Fermi distribution describes the hot spot from the time of fusion. At least, the experimental evidence does not contradict this assumption.

In the present work the effect of the initial exciton number on the PEQ neutron emission has been studied. In Fig. 3 we have compared the angular variation of the neutron yield at two different values of the initial excited particles f_0. The solid line is the calculated value with f_0 calculated by Eq. (10) while the dashed line is that for $f_0=A_P$, the number of nucleons in the projectile particle. This second choice gives a large overprediction at 0° and 30° while there is very little change for 60°. This is because at 60° emission angle and for the incident energy considered here, the PEQ contribution is very small as is evident from Fig. 1, whereas at for-

ward angles high energy PEQ emissions have significant contributions. From Eq. (5) we see that the total PEQ neutron cross section depends on the number of excited neutrons at different stages N. Here we have considered emissions from $N=0$ only and thus the number of excited particles is equal to f_0. For $f_0=A_P$, the number of excited neutrons at $N=0$ is $A_P-Z_P=8$, which is larger than when f_0 is calculated by Eq. (10), which is 5.7. This explains the overprediction of the calculated values with $f_0=A_P$. This observation also helps us to conclude that between the two methods, calculations based on the momentum sphere consideration are close to reality, which was not clear in our earlier analysis [4].

We would like to point out that in the present calculations, we have ignored the effect of nuclear temperature on the collision rates or mean free paths of the interacting nucleons. That is, while using Eq. (12) to calculate the collision rate, we have used $k=1$ throughout. A more rigorous approach would be to consider temperature dependent collision rates or mean free paths by making k dependent on the temparature. In the present model, this will introduce a difference in the PEQ emission probabilities from the hot spot and the cold spot. However, introduction of temperature dependence in the collision rate will involve significant computational complexities. Since, in the present case, PEQ emission seems to take place only from a single stage ($N=0$), we have postponed such calculations as a subject for future studies.

V. CONCLUSION

We have made measurements and analyses of thick-target neutron yield distributions from $^{16}O+^{181}Ta$ reaction at 7.2A MeV, which is almost the threshold energy to observe the PEQ emissions. Calculated results from an earlier developed model [4] fit the experimental results well. Analyses of the results reveal that at such low energies PEQ emissions are possible only before target and projectile nucleons start interacting by scattering. This situation would suggest that PEQ emission will not occur at such low energies for nucleon induced reactions.

[1] P.K. Sarkar, T. Bandyaopadhyay, G. Muthukrishnan, and Sudip Ghosh, Phys. Rev. C **43**, 1855 (1991).

[2] T. Kurosawa, T. Nakamura, N. Nakao, T. Shibata, Y. Uwamino, and A. Fukumura, Nucl. Instrum. Methods Phys. Res. A **430**, 400 (1999).

[3] T. Kurosawa, N. Nakao, T. Nakamura, Y. Uwamino, T. Shibata, N. Nakanishi, A. Fukumura, and K. Murakami, Nucl. Sci. Eng. **132**, 30 (1999).

[4] Maitreyee Nandy, Sudip Ghosh, and P.K. Sarkar, Phys. Rev. C **60**, 044607 (1999).

[5] P.K. Sarkar and Maitreyee Nandy, Phys. Rev. E **61**, 7161 (2000).

[6] Y. Uwamino, K. Shin, M. Fujii, and T. Nakamura, Nucl. Instrum. Methods Phys. Res. **204**, 179 (1982).

[7] F. Ziegler, J. P. Bieserk, and U. Littmark, *The Stopping and Ranges in Solids* (Pergamon, New York, 1985).

[8] M. Blann, LLNL Report No. UCID 19614, 1982 (unpublished); ICTP Workshop Report No. SMR/284-1, 1988 (unpublished).

[9] A. De, S. Ray, and S.K. Ghosh, J. Phys. G **11**, L79 (1985).

[10] W.W. Wilke, J.R. Birkelund, H.J. Wollersheim, A.D. Hoover, J.R. Huizenga, W.U. Schroder, and L.E. Tubbs, At. Data Nucl. Data Tables **25**, 391 (1980).

[11] G.S.F. Stephans, D.G. Kovar, R.V.F. Janssens, G. Rosner, H. Ikezoe, B. Wilkins, D. Henderson, K.T. Lesko, J.J. Kolata, C.K. Galbke, B.V. Jacak, Z.M. Koenig, G.D. Westfall, A. Szanto de Toledo, E.M. Szanto, and P.L. Gonthier, Phys. Lett. **161B**, 60 (1985); A. Iwamoto, Phys. Rev. C **35**, 984 (1987); E. Fabrici, E. Gadioli, E. Gadioli Erba, M. Galmarini, F. Fabbri, and G. Reffo, *ibid.* **40**, 2548 (1989).

[12] M. Blann, Phys. Rev. C **35**, 1581 (1987).

[13] M. Blann and H.K. Vonach, Phys. Rev. C **28**, 1475 (1983).

[14] A. Chatterjee, K.H.N. Murthy, and S.K. Gupta, Pramana **16**, 391 (1981).

[15] M. Blann, Phys. Rev. Lett. **27**, 337 (1971).

[16] N. Chakravarty, P.K. Sarkar, Maitreyee Nandy, and Sudip Ghosh, J. Phys. G **24**, 151 (1998).